Neuroscience Letters 597 (2015) 104–110

Contents lists available at ScienceDirect

Neuroscience Letters

journal homepage: www.elsevier.com/locate/neulet

Research article

Silent suppressive surrounds and optimal spatial frequencies of single neurons in cat V1

Tao Xu[a,b], Hong-Mei Yan[a], Xue-Mei Song[b,*], Ming Li[c], Yong-Jie Li[a]

[a] Key Laboratory for Neuroinformation of Ministry of Education, University of Electronic Science and Technology of China, Chengdu, China
[b] Shanghai Institutes of Biological Sciences, Chinese Academy of Sciences, Shanghai, China
[c] The College of Mechatronics and Automation, National University of Defense Technology, Changsha, China

HIGHLIGHTS

- SS neurons prefer significantly higher SFs than SN neurons do.
- The end and side inhibition neurons prefer the highest SFs.
- The correlation was stronger between the optimal SFs and end vs. side suppression.

ARTICLE INFO

Article history:
Received 31 December 2014
Received in revised form 21 April 2015
Accepted 23 April 2015
Available online 25 April 2015

Keywords:
Primary visual cortex (V1)
Spatial frequency (SF)
Surround- suppressive (SS)
Surround-non-suppressive (SN)

ABSTRACT

The receptive fields of the clear majority of neurons in the primary visual cortex (V1) of cats contain silent surround regions beyond the classical receptive field (CRF). When stimulated on their own, the silent surround regions do not generate action potentials (spikes); instead, they modulate (and usually partially suppress) spike responses to stimuli presented in the CRF. In the present study, we subdivided our sample of single V1 neurons recorded from anesthetized cats into two distinct categories: surround-suppressive (SS) cells and surround-non-suppressive (SN) cells. Consistent with previous reports, we found a negative correlation between the size of the CRF and the optimal spatial frequency (SF) of circular patches of achromatic gratings presented in the cells' receptive fields. Furthermore, we found a positive correlation between the strength of the surround suppression and the optimal spatial frequency of the achromatic gratings presented in the cells' receptive fields. The correlation between the strength of surround suppression and the optimal spatial frequency was stronger in neurons with suppressive regions located in the so-called 'end' zones. The functional implications of these relationships are discussed.

1. Introduction

In the primary visual cortex (V1), neuronal responses to stimuli presented to the classical receptive field (CRF) can be modulated by stimuli surrounding the CRF [1–6]. The surround field is conventionally referred to as the "non-classical receptive field" (nCRF). Previous studies have suggested that the center responses of the majority of V1 cells are suppressed by the inclusion of surround stimuli. We named these neurons "surround-suppressive" (SS) cells [7].

However, not all V1 cells are suppressed by surround stimuli. Instead, in some cells, responses will saturate and exhibit a plateau-like tuning profile [1,4]. These cells we named "surround-non-suppressive" (SN) cells [7].

A correlation between the optimal SF and the minimum response field (mRF) has been reported [8–10]. The SF tuning characteristics at different visual topographical locations in the cat V1 have also been studied [11,12]. However, the relationship between optimal SF and surround summation properties is seldom investigated.

Previous electrophysiological studies [1,2,5,13] have shown that the modulatory influences from the side and end sub-regions of the nCRF can be similar or different for different cells. Using the abbreviation "s" for suppressive and "n" for non-suppressive, four possible combinations of the integration of the side (width, *W*) and end (length, *L*) can be defined: (A) *Ls*/*Ws*, (B) *Ln*/*Wn*, (C) *Ls*/*Wn*, and (D) *Ln*/*Ws*. Of the four types of combinations, type A accounts for

* Corresponding author at: Shanghai Institutes of Biological Sciences, Chinese Academy of Sciences, 320 Yue-Yang Road, Shanghai 200031, China.
Tel.: +86 21 54920312; fax: +86 21 54921778.
E-mail address: xmsong@sibs.ac.cn (S. Xue-Mei).

http://dx.doi.org/10.1016/j.neulet.2015.04.039
0304-3940/

the majority of cells [1,5]. Their feature-selective surround inhibition constitutes the neural basis of perceptual 'pop out' [14,15] and contour discrimination [5,7,10,13,16]. We, therefore, studied the optimal SF of this type of neuron and explored the various influences of end and side inhibition on optimal SF.

In this study, we recorded the single-unit activities and determined the optimal SF of neurons with different surround summation properties. We found that in cat V1, SS neurons preferred higher SFs than SN neurons did, and the correlation between the strength of surround suppression, and optimal SFs was stronger in neurons with end suppression than in neurons with side suppression. From these results, we propose that SFs have roles not only in the scale-invariant properties of visual information processing but also in perceptual processing. For surround inhibition, end inhibition may play more important roles than side inhibition in perception.

2. Materials and methods

2.1. Animal preparation

This study was performed in strict accordance with the recommendations contained in the Guide for the Care and Use of Laboratory Animals from the National Institutes of Health. The protocol was specifically approved by the Committee on the Ethics of Animal Experiments of the Shanghai Institute for Biological Sciences, Chinese Academy of Sciences (Permit Number: ER-SIBS-621001C). Adult cats of both sexes were used for these experiments. Surgical procedures and animal preparation have been described previously [7].

2.2. Single-unit recordings

Extracellular recordings were made using tungsten-in-glass microelectrodes. The electrodes were advanced into the cortex using a step-motor micro-drive (Narishige, Japan), with the vertical angle penetrating through the cortical layers. Only well-isolated cells satisfying strict criteria for single-unit recordings were collected for further analyzes.

2.3. Visual stimulation

Visual stimuli were generated by a Cambridge Systems VSG graphics board. The stimuli were patches of drifting sinusoidal gratings presented on a high-resolution monitor (40 cm × 30 cm) with a 100 Hz vertical refresh rate. The screen was maintained at the same mean luminance as the stimulus patches (10 cd/m^2). The monitor was placed 57 cm from the cat's eyes.

2.4. Procedures

Once the single-cell action potentials were isolated, we measured the cell's orientation tuning, spatial and temporal frequency tuning, and response function. Each cell was stimulated monocularly through the dominant eye and characterized by measuring its response to drifting sinusoidal gratings.

The method used to define the center of the CRF was the same as that described by Song and Li [17] and Xu et al. [7]. Once the center of each cell's receptive field and the excitatory receptive field were identified, the orientation tuning of the neuron was re-assessed with a 40% contrast grating at a fixed diameter of the CRF. Next, the optimal spatial frequency was determined by presenting ~10° gratings at the preferred orientation while varying the spatial period.

In the size-tuning tests, the circular sinusoidal gratings (40% contrast) were centered over the receptive field and randomly presented with different diameters (from 0.1° to 20°). The optimized values of these parameters (orientation, spatial and temporal frequency) were used in these tests. We defined the CRF size as the aperture size of the peak response diameter (the stimulus diameter at which the response was maximal if the responses decreased at larger stimulus diameters or the stimulus diameter at which the response reached 95% of the peak value if they did not).

To obtain quantitative estimates of the length and width of a cell's excitatory response field, we measured the length and width summation curves and used standard procedures to fit curves to the experimental data [1].

Cells were classified as simple if the ratio of F1/DC was >1 and complex if not [18].

2.5. Data analysis and statistical analysis

The size-tuning curves for all recorded cells were fit using a DOG model [1]. The model was defined by the following equation:

$$R(s) = R_0 + K_e \int_{-s/2}^{s/2} e^{-(2y/a)^2}\,dy - k_i \int_{-s/2}^{s/2} e^{-(2y/b)^2}\,dy \quad (1)$$

where R_0 is the spontaneous firing rate, and each integral represents the relative contribution from putative excitatory and inhibitory components. The excitatory Gaussian is described by gain, K_e, and a space constant, a, and the inhibitory Gaussian by its gain, K_i, and space constant, b. All population values shown below are presented as the mean ± SEM.

In the spatial frequency-tuning experiments, we used ~10° drifting gratings with an optimal orientation and temporal frequency to stimulate cell responses. Cells' responses were recorded to ten gratings of different spatial frequencies, which were evenly distributed between 0.1 and 1 cycle/deg. Then, we fit the data with a DOG (difference of Gaussians) model by minimizing the squared error between the DOG curve and the data [19], with all parameters (R_0, K_e, μ_e, σ_e, K_i, μ_i, and σ_i) free.

$$R(SF) = R_0 + K_e \exp\left(\frac{-(SF-\mu_e)^2}{2\sigma_e^2}\right) - K_i \exp\left(\frac{-(SF-\mu_i)^2}{2\sigma_i^2}\right) \quad (2)$$

All data are expressed as the mean ± SD. All two-way comparisons were tested for significance using the Mann–Whitney U test.

3. Results

Stable single-cell recordings were obtained from 201 neurons in cat V1. All had receptive fields centered within 10° of the visual axis.

3.1. Two types of surround modulation

Based on the fitted area-summation curves, cells could be classified into two types: surround-suppressive (SS) neurons and surround-non-suppressive (SN) neurons (Fig. 1A and B). The majority of the neurons (149) was SS, meaning that their responses increased to a peak and then decreased as the stimulus diameter increased further. The minority of neurons (52) were SN, meaning that their spike rates rose with increasing stimulus diameter and then reached an asymptote. CRF size was defined as the peak response diameter (as in Fig. 1A) or as the diameter of the saturation point (reaching 95% of the peak value, as in Fig. 1B). We quantified the degree of surround suppression for each cell using the SI (1-asymptotic response/peak response).

Liu et al. [20] described a third group of surround-modulated neurons, the facilitative cells, and showed that most of these neurons were located in the infragranular layers. We recorded only

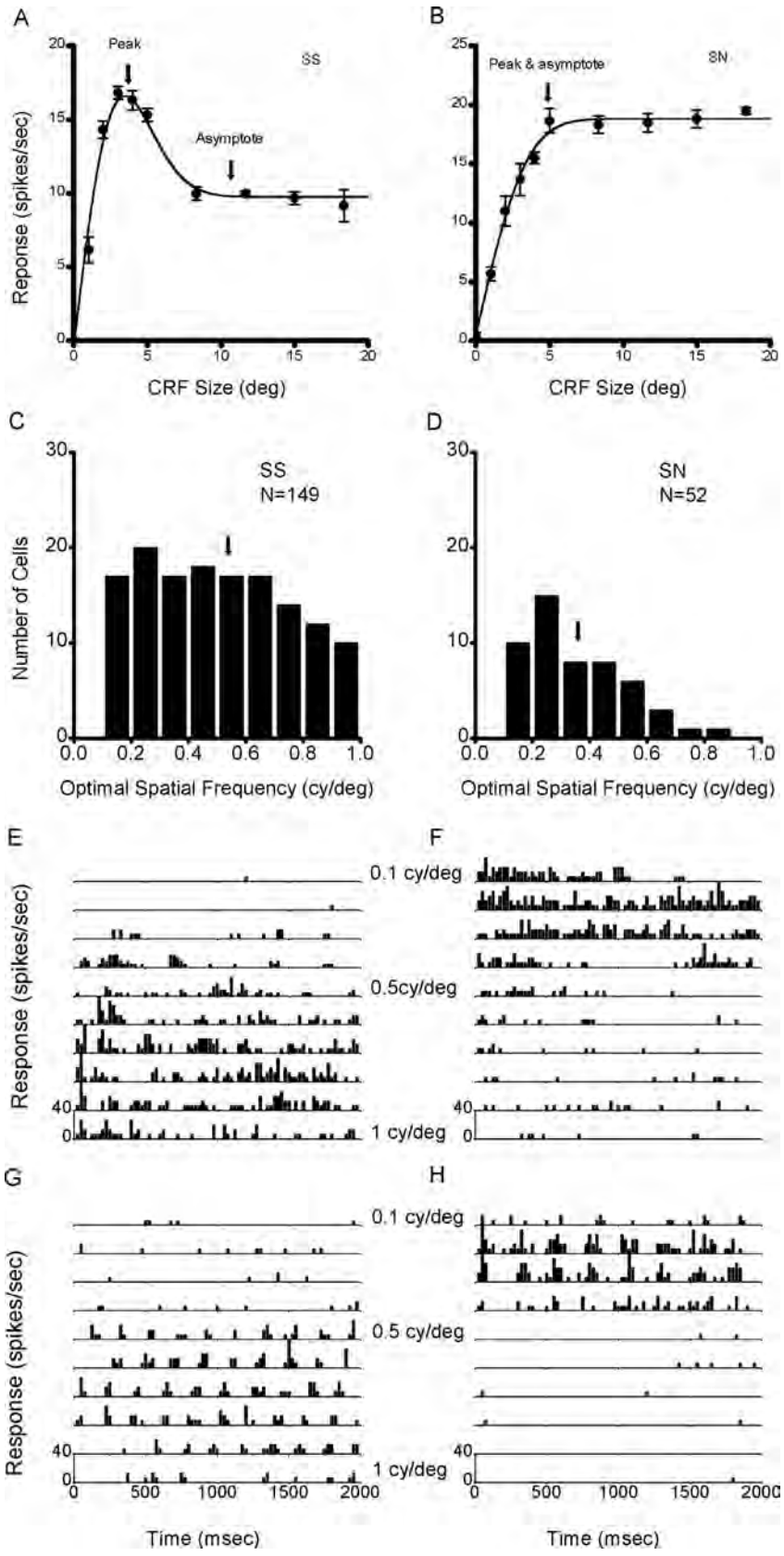

Fig. 1. Size-tuning curves for two representative cells (SS, SN), PSTH responses to variations in the spatial period for four typical cells and the distribution of optimal SFs for SS and SN cells.

(A) A neuron with suppressive surround (SI = 0.41). (B) A cell showing a non- suppressive surround (SI = 0). The arrows indicate the stimulus diameter at which the responses were maximal and/ or became asymptotic. Error bars: ± SEM.

(C) Distribution of the optimal SFs for surround-suppressive (SS) cells. (D) Distribution of the optimal SFs for surround-non-suppressive (SN) cells. The arrows indicate the mean optimal SF. (E)–(H) show the PSTH responses of SS-complex, SN-complex, SS-simple, SN-simple cells, respectively, to variations in spatial period.

three cells of this type and so did not conduct an analysis of this type of neuron.

3.2. Optimal SF of SS and SN neurons

We compared the optimal SF of SS and SN neurons. The optimal SFs of 149 SS neurons showed a wide distribution from 0.1 to 1.0 cycles/deg (mean = 0.53 ± 0.26) (Fig. 1C), and the optimal SFs of 52 SN neurons distributed mostly around the low frequency range (Fig. 1D) (mean = 0.37 ± 0.19). The difference between the two groups of neurons was significant ($P < 0.001$). PSTH responses to the stimulation of various spatial frequencies are shown for four typical cells in Fig. 1E–H.

Teichert et al. [21] showed that in macaque V1 neurons, CRF size reflects the area in the visual field used to shape SF selectivity. Accordingly, we compared CRF size between SS and SN neurons. The CRFs of SN neurons (5.7° ± 2.3°) were significantly larger ($P < 0.001$) than the CRFs of SS neurons (3.8° ± 2.3°). Consequently, information regarding different SFs might be processed by different types of neurons in V1.

3.3. Dependence on cortical depth

Due to uncertainty regarding the exact laminar position of our recording sites, we assigned a laminar location by pooling those neurons estimated to be in the superficial layers (<600 μm), the intermediate layers (600–1200 μm) and the deep layers (>1200 μm). The majority of the cells (158) was recorded in the superficial and intermediate layers. We found that SS and SN neurons were distributed evenly across all cortical layers (Fig. S1) and that neurons in the intermediate layers had the greatest optimal SFs, whereas, those in the deep layers had the lowest (Fig. S1). We also found that the mean optimal SF of simple cells (0.44 ± 0.23, $n = 73$, Fig. S2A) was lower than that of complex cells (0.51 ± 0.26, $n = 128$, Fig. S2B). However, this difference was not significant ($P = 0.06$).

Supplementry material related to this article found, in the online version, at http://dx.doi.org/10.1016/j.neulet.2015.04.039.

3.4. The relationship between optimal SF and the strength of surround suppression

We further explored the relationship between optimal SF and the strength of surround suppression. Scatter plots of optimal SF vs. SI are shown in Fig. 2A for 149 SS neurons. We found a positive correlation ($r = 0.33$, $P < 0.001$) between the two values. Although the correlation was not strong, this result may indicate that the optimal SF is higher for SS neurons with stronger surround suppression. Fig. 2B shows the relationship between optimal SF and the size of the CRF. There was a strong negative correlation ($r = -0.61$, $P < 0.001$) between optimal SF and the size of the CRF, which is consistent with the results of Teichert et al. [21] in macaque V1.

3.5. Optimal SF of the Ls/Ws, Ln/Wn, Ls/Wn, and Ln/Ws neurons

The optimal SF of *Ls*/*Ws* ($n = 104$), *Ln*/*Wn* ($n = 19$), *Ls*/*Wn* ($n = 40$) and *Ln*/*Ws* ($n = 38$) neurons are shown in Fig. 3A–D, respectively. The *Ls*/*Ws* neurons had the highest SFs (0.57 ± 0.26), which differed significantly from the SFs of the other three types of neurons (*Ln*/*Wn*: 0.36 ± 0.20, $P < 0.001$; *Ls*/*Wn*: 0.42 ± 0.25, $P = 0.002$; *Ln*/*Ws*: 0.40 ± 0.21, $P < 0.001$). In our data, the CRFs of the *Ls*/*Ws* neurons were the smallest (3.5° ± 2.4°) and differed significantly from the CRFs of the *Ln*/*Wn* (5.8° ± 2.3°, $P < 0.001$), *Ls*/*Wn* (4.6° ± 2.6°, $P = 0.01$) and *Ln*/*Ws* (5.7° ± 2.3°, $P < 0.001$) neurons, which could be the reason for the high spatial frequency preference in the *Ls*/*Ws* neurons.

3.6. The relationship between length (or width) summation properties and the optimal SF

Among the four types of combinations, the *Ls*/*Ws* type accounted for the majority of neurons [1,2], and this type of surround inhibition is viewed as being the neural basis of perceptual 'pop out'. Therefore, we explored the various influences of end and side inhibition on optimal SF. Scatter plots of optimal SF vs. SI for length and width are shown in Fig. 4A and B, respectively. The two values were correlated in both cases, but the correlation was stronger in the end-stopping cells ($r = 0.31$, $P < 0.001$) than in the side-stopping cells ($r = 0.18$, $P < 0.001$).

The relationships between optimal SF vs. CRF for length and width are shown in Fig. 4C and D, respectively. There was a

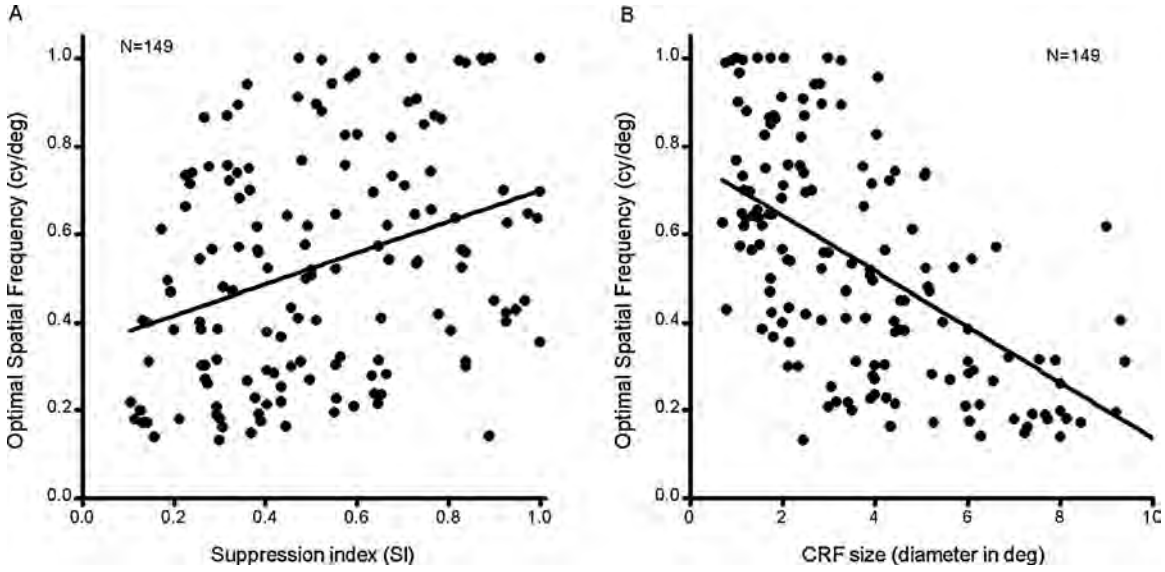

Fig. 2. Relationship between optimal SF and spatial summation properties in SS neurons.
(A) Relationship between optimal SF and value of SI for the SS neurons. (B) Relationship between optimal SF and size of CRF for the SS neurons.

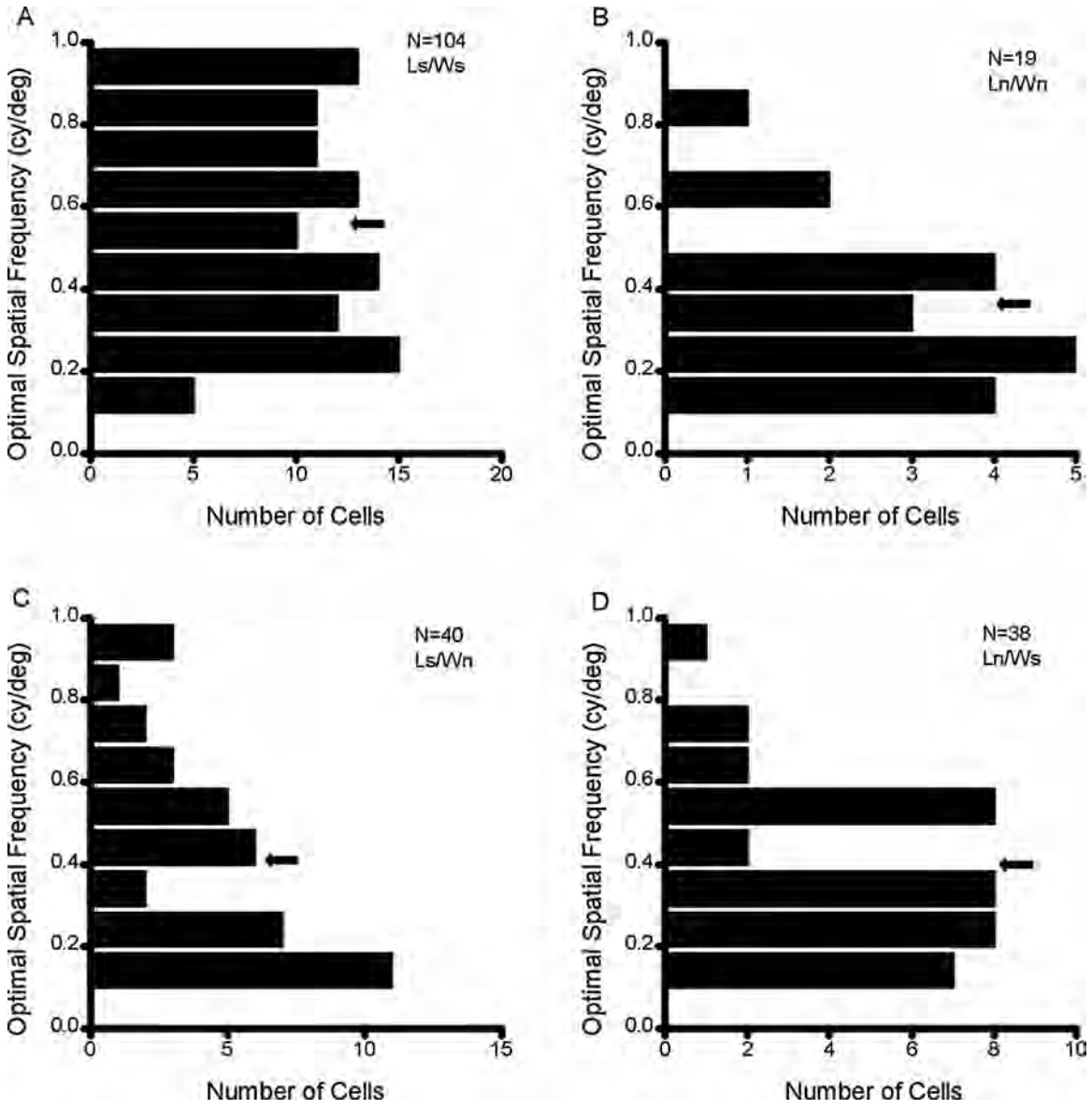

Fig. 3. Distribution of optimal SF for the four cell types.
(A)–(D) show the distributions of the optimal SF in the *Ls*/*Ws*, *Ln*/*Wn*, *Ls*/*Wn*, and *Ln*/*Ws* neurons, respectively. The arrows indicate the mean PeakSF of each type.

negative correlation in both cases, but the correlation coefficient was larger between optimal SF and CRF length ($r = -0.54$, $P < 0.001$) than between optimal SF and CRF width ($r = -0.39$, $P < 0.001$).

4. Discussion

4.1. Possible explanations for the higher SF in SS neurons and lower SF in SN neurons

X-type cells in the cat lateral geniculate nucleus (LGN) and V1 neurons with suppressive surrounds generally prefer higher SFs, whereas, Y-type LGN cells and V1 neurons with non-suppressive surrounds prefer lower SFs [22]. Both X- and Y-type neurons project to cat V1, with differences in the laminar termination of axons [23]. We did not observed any differences in the distribution of SS and SN neurons in V1 across cortical layers, which is consistent with a previous report [20]. However, in the two studies, the method of assigning cells to cortical layers was based on recording depth and not on histological verification. We found that neurons in intermediate layers had the highest optimal SFs, whereas, those in the deeper layers had the lowest, which is not in agreement with the results of Tolhurst and Thompson [24] (using histological verification). Therefore, it would be worthwhile to further analyze the laminar distribution of SS and SN neurons in V1 using a more precise method.

4.2. Possible reasons for the highest SFs in Ls/Ws *neurons*

Teichert et al. [21] presented evidence to support the hypothesis that CRF size reflects the area in the visual field used to shape SF selectivity. Studies of cat V1 [25–27] reported a smaller variation in CRF size with different contrasts and/or SFs. In the study presented here, we found that the size of CRFs of *Ls*/*Ws* neurons were the smallest and differed significantly from the size of the CRFs of the *Ln*/*Wn*, *Ls*/*Wn*, and *Ln*/*Ws* neurons, which might be the reason for the highest SFs in the *Ls*/*Ws* neurons.

Tailby et al. [25] investigated the relationship between surround suppression and SF by measuring area-summation tuning curves at several SFs in cat and monkey V1. They found that the degree of surround suppression was stronger at higher SFs. In our study, we

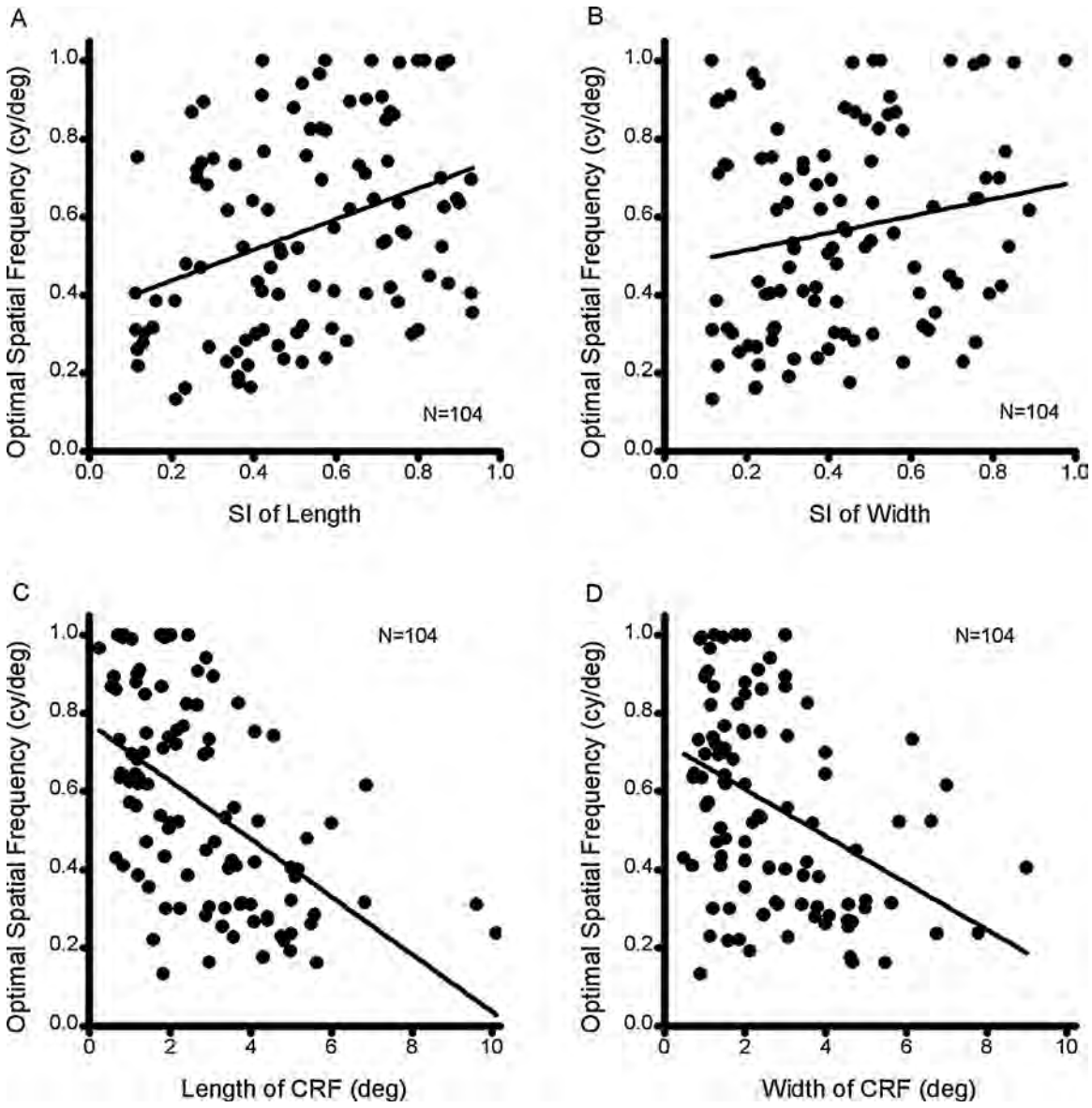

Fig. 4. Relationship between end (or side) summation and optimal SF.
The relationships between optimal SF and length or width SI are shown in (A) and (B). The relationships between optimal SF vs. CRF length or width are shown in (C) and (D).

found a positive relationship between SI and optimal SF (shown in Fig. 2A). These results indicate that the suppressive area outside the CRF might not contribute to the shaping of SF tuning [21], whereas, the responses of *Ls*/*Ws* neurons in V1 could be dependent on high-SF stimuli.

4.3. *Physiological roles of high SF in* Ls/Ws *neurons*

Surround suppression in V1 has been traditionally considered to be a neural substrate for figure-ground segregation in perception [3,6,28]. Walker et al. [13] reported the occurrence of asymmetric suppression outside the CRF in cat V1. End stopping could provide a means to detect the termination of a line segment [29] and could be used to detect curvature [30,31]. However, cells with side suppression would be poor detectors of curvature or line termination. A recent study [32] incorporated a model that simulated the behavior of V1 neurons with respect to adaptive end inhibition, and this model suggested that additional physiological experiments should focus on the analysis of the strength of inhibition coming from different regions, especially from the end regions. In our study, we showed that the correlation between the strength of surround suppression and optimal SF was stronger in neurons with length suppression than in neurons with width suppression. Moreover, the correlation between SF and the size of the CRF was stronger in the longitudinal direction than in the width direction.

In conclusion, our results demonstrate that (1) SS neurons preferred higher SFs, whereas, SN neurons preferred lower SFs; (2) *Ls*/*Ws* cells had the highest optimal SF, which differed significantly from the optimal SFs of the other three types of cells (*Ln*/*Wn*, *Ls*/*Wn*, and *Ln*/*Ws*); and (3) for *Ls*/*Ws* neurons, the correlation was stronger between optimal SF and length summation properties, whereas, the relationship was weaker between optimal SF and width summation properties.

Acknowledgments

This work was supported by the Major State Basic Research Program (2013CB329401), the Natural Science Foundations of China (91420105, 91120013, 61105116, 61375115), and the Shanghai

Municipal Committee of Science and Technology (088014158, 098014026).

We thank Dr D.A. Tigwell for comments on the manuscript and X.Z. Xu for technical assistance. We are grateful to the editor and reviewers for helpful suggestions on this manuscript.

References

[1] G.C. DeAngelis, R.D. Freeman, I. Ohzawa, Length and width tuning of neurons in the cat's primary visual cortex, J. Neurophysiol. 7 (1994) 347–374.
[2] C.Y. Li, W. Li, Extensive integration field beyond the classical receptive field of cat's striate cortical neurons-classification and tuning properties, Vision Res. 34 (1994) 2337–2355.
[3] A.M. Sillito, K.L. Grieve, H.E. Jones, J. Cudeiro, J. Davis, Visual cortical mechanisms detecting focal orientation discontinuities, Nature 378 (1995) 492–496.
[4] F. Sengpiel, A. Sen, C. Blakemore, Characteristics of surround inhibition in cat area 17, Exp. Brain Res. 116 (1997) 216–228.
[5] H.S. Yao, C.Y. Li, Symmetry and spatial summation properties of the integration field of cat's striate cortical neurons, Acta Biophys. Sin. 14 (1998) 493–500.
[6] P. Series, J. Lorenceau, Y. Fregnac, The silent surround of V1 receptive fields: theory and experiments, J. Physiol. Paris 97 (2003) 453–474.
[7] T. Xu, L. Wang, X.M. Song, C.Y. Li, The detection of orientation continuity and discontinuity by cat V1 neurons, PLoS One 8 (2013) e79723.
[8] D. Hubel, T. Wiesel, Receptive fields, binocular interaction and functional architecture in the cat's visual cortex, J. Physiol. 160 (1962) 106–154.
[9] D. Hubel, T. Wiesel, Receptive fields and functional architecture of monkey striate cortex, J. Physiol. 195 (1968) 215–243.
[10] R. De Valois, D. Albrecht, L. Thorell, Spatial frequency selectivity of cells in macaque visual cortex, Vis. Res. 22 (1982) 545–559.
[11] H. Ikeda, M.J. Wright, Spatial and temporal properties of 'sustained' and 'transient' neurons in area 17 of the cat's visual cortex, J. Physiol. 22 (1975) 363–383.
[12] H.B. Yu, T.D. Shou, Spatial frequency tuning characteristic of cat primary visual cortex at different topological location by optical imaging, Acta Physiol. Sin. 52 (2000) 411–415.
[13] G.A. Walker, I. Ohzawa, R.D. Freeman, Asymmetric suppression outside the classical receptive field of the visual cortex, J. Neurosci. 19 (1999) 10536–10553.
[14] M.K. Kapadia, M. Ito, C.D. Gilbert, G. Westheimer, Improvement in visual sensitivity by changes in local context: parallel studies in human observers and in V1 of alert monkeys, Neuron 15 (1995) 843–856.
[15] V.A.F. Lamme, The neurophysiology of figure-ground segregation in primary visual cortex, J. Neurosci. 15 (1995) 1605–1615.
[16] W.F. Xu, Z.M. Shen, C.Y. Li, Spatial phase sensitivity of V1 neurons in alert monkey, Cereb. Cortex 15 (2005) 1697–1702.
[17] X.M. Song, C.Y. Li, Contrast-dependent and contrast-independent spatial summation of primary visual cortical neurons of the cat, Cereb. Cortex 18 (2008) 331–336.
[18] B.C. Skottun, R.L. DeValois, D.H. Grosof, J.A. Movshon, D.G. Albrecht, A.B. Bonds, Classifying simple and complex cells on the basis of response modulation, Vis. Res. 31 (1991) 1079–1086.
[19] W. Zhu, D.J. Xing, M. Shelley, R. Shapley, Correlation between spatial frequency and orientation selectivity in V1 cortex: implication of a network model, Vis. Res. 50 (2010) 2261–2273.
[20] Y.J. Liu, H.N. Maziar, D.C. Lyon, Dynamics of extraclassical surround modulation in three types of V1 neurons, J. Neurophysiol. 105 (2011) 1306–1317.
[21] T. Teichert, T. Wachtler, F. Michler, A. Gail, R. Eckhorn, Scale-invariance of receptive field properties in primary visual cortex, BMC Neurosci. 8 (2007) 38.
[22] A.M. Derington, A.F. Fuchs, Spatial and temporal properties of X and Y cells in the cat lateral geniculate nucleus, J. Physiol. 293 (1979) 347–364.
[23] T.F. Freund, K.A. Martin, D. Whitteridge, Innervation of cat visual areas 17 and 18 by physiologically identified X- and Y- type thalamic afferents I. arborization patterns and quantitative distribution of postsynaptic elements, J. Comp. Neurol. 242 (1985) 263–274.
[24] D.J. Tolhurst, I.D. Thompson, On the variety of spatial frequency selectivities shown by neurons in area 17 of the cat, Proc. R. Soc. 213 (1981) 183–199.
[25] C. Tailby, S.G. Solomon, J.W. Peirce, A.B. Metha, Two expressions of 'surround suppression' in V1 that arise independent of cortical mechanisms of suppression, Vis. Neurosci. 24 (2007) 99–109.
[26] C. Wang, C. Bardy, J.Y. Huang, T. FitzGibbon, B. Dreher, Contrast dependence of center and surround integration in primary visual cortex of the cat, J. Vis. 9 (2009) 1–15.
[27] K. Chen, X.M. Song, C.Y. Li, Contrast-dependent variations in the excitatory classical receptive field and suppressive nonclassical receptive field of cat primary visual cortex, Cereb. Cortex 23 (2013) 283–292.
[28] K. Zipser, V.A.F. Lamme, P.H. Schiller, Contextual modulation in primary visual cortex, J. Neurosci. 16 (1996) 7376–7389.
[29] B. Julesz, Textons, the elements of texture perception, and their interactions, Nature 290 (1981) 91–97.
[30] A. Dobbins, S.W. Zucker, M.S. Cynader, Endstopped neurons in the visual cortex as a substrate for calculating curvature, Nature 329 (1987) 438–441.
[31] A. Dobbins, S.W. Zucker, M.S. Cynader, Endstopping and curvature, Vis. Res. 29 (1989) 1371–1387.
[32] C. Zeng, Y.J. Li, C.Y. Li, Center-surround interaction with adaptive inhibition: a computational model for contour detection, NeuroImage 55 (2011) 49–66.